



Numerical simulation of infrasound perception, with reference to prior reported laboratory effects.

M.A.Swinbanks^{a)}
MAS Research Ltd,
8 Pentlands Court,
Cambridge UK CB4 1JN

In earlier presentations, the author has argued that conventional assessments of the perception of infrasound based on mean (rms derived) sound energy levels underestimate the importance of the associated crest factor of very low frequency sound pressure variations. By simulating the dynamic response of the ear at levels close to the hearing threshold, it is apparent that infrasound may be perceptible at lower levels than those based on long time constant rms assessment. In particular, it will be shown that the existence of a finite threshold of audibility, together with the added presence of low level higher frequency noise in the first critical band (i.e. below 100Hz), can imply the perception of infrasound at significantly lower levels than has hitherto been acknowledged. The results of simulations will be compared to independently reported effects which have been observed in laboratory testing by other researchers.

1 INTRODUCTION

Hitherto, methods of assessing infrasound perception have tended to rely on visual comparison of the low frequency spectrum, either 1/3rd octave or narrow band, with the low frequency threshold of hearing. This approach is not satisfactory, because as shown by Pedersen¹, individual spectral levels vary according to the chosen measurement bandwidth. Essentially, such a comparison is not one of like-with-like. The threshold of hearing is determined experimentally by presenting single individual tones to a test subject, and establishing the level at which such tones first become audible. In contrast, sound encountered in practice often consists of a multiplicity of simultaneous components, both broadband noise and multiple tones or harmonics. Under such circumstances, the assessment of perception or audibility is necessarily more complex.

^{a)} email: malcva@msn.com

To address this problem, Pedersen proposed first weighting the spectrum with a frequency function corresponding to the inverse hearing threshold – essentially accounting for the transmission of sound to the hair cell detection system of the inner ear. Under this transformation, the hearing threshold itself now assumes a constant value, at 0dB, and enables the different components at different frequencies to be assessed on a common basis. He then proposed that by integrating the resultant spectral energy over the first and second critical bands of hearing, two specific energy levels could be determined which are now uniquely defined, and independent of the precise resolution bandwidth. By comparing these energy levels with the 0dB threshold, he could then determine when the sound energy in each of these two critical bands exceeds this threshold, and consequently becomes perceived.

The lowest critical band of hearing contains a wealth of detail - the infrasound regime, the very low frequency regime, and moderately low frequencies up to 100Hz. Defining only a single number for this entire critical band fails to provide any information as to where within this overall range the sound first becomes perceptible. The present author therefore proposed² that instead of defining a single integrated value for the entire frequency band, a running integration should be performed starting from the very lowest frequencies and progressively broadening the range of integration. In this way, a unique cumulative ascending curve is derived, which is independent of the original measurement bandwidth. Intersection of this curve with the 0dB threshold defines the lowest frequency at which the integrated energy equates to the equivalent energy of a single sinusoidal test tone. Such a procedure provides a first estimate of the frequency at which the sound would be expected to become perceptible.

The author argued, however, that a pure sinusoidal test tone has a low crest factor, while more complex sound signals often possess higher crest factors, with the result that they may penetrate the threshold even though their mean square energy is less than 0dB. For example, periodic impulsive noise consists of multiple harmonically related components which add together coherently, rather than as random independent components combined in mean square. He proposed that such crest factor effects could be addressed by passing the digitized sound signal through a time domain simulation of the hearing transfer function. By comparing the resultant output levels with the constant amplitude limits of the transformed hearing threshold, audibility could be determined. Examples of such analyses compared favorably with prior experimental reporting of the audibility of both broadband and periodic impulsive signals.

The simulation and analyses described so far represent entirely linear processes. In contrast, the existence of a defined, finite hearing detection threshold implies that non linear effects may be manifest at very low sound levels. As a consequence, components of sound that would be fully independent according to linear analysis may then become coupled. Under such circumstances the presence of one component of sound could serve to enhance the perception of another. The purpose of this paper is to extend the prior numerical simulation to include such a process, and to consider the possible resultant effects.

2 NUMERICAL MODEL

The hearing process was modeled in the time-domain by two successive processes, with properties as follows. The inverse hearing threshold was simulated by a 5-pole, 6-zero ARMA (autoregressive moving-average) filter, sampled at 1kHz, whose frequency response is shown in Fig 1a compared to the median low-frequency inverse threshold. The precision of fit is well within the tolerance of experimental measurement of this threshold. The output of this filter

was then subject to a threshold operation as shown in Fig 1b. It is assumed that for amplitudes above the threshold value, the output is linearly related to the input, but that below the threshold the output goes completely to zero. Three possible versions of the threshold transition were considered, as shown in this figure. The simplest transition is a sharp cut-off at the threshold value, with the output going immediately to zero below this value. A second possibility is that individual sensing hair cells do not respond at exactly the same value, so that an average, more tapered cut-off takes place either side of the threshold. Thirdly, it is possible that the subsequent output above the threshold rises linearly from zero at reduced overall level, rather than reverting immediately to the full linear input value.

When a slowly increasing sinusoidal tone is passed through such a threshold, it does not immediately form a full-wave output. As the amplitude increases from zero, initially only the positive and negative peaks of the waveform are transmitted. Subsequently at higher amplitudes more of the waveform is transmitted until ultimately the full waveform is reproduced. Fig 1c shows the output amplitude in decibels, as a function of the decibel level of a sine wave input, for each of the three threshold configurations. It can be seen that the cut-on is always a progressive process, with different degrees of severity according to the specific threshold implementation. The precise parameters of each threshold were chosen empirically, so that there was reduced but finite amplitude at 0dB, and directly comparable attenuation immediately below 0dB.

Analysis of more complex waveforms shows that in practice, the output is largely insensitive to the difference between these three implementations. The following numerical examples therefore assume a sharp cut-off corresponding to the red characteristic of Fig 1b. To illustrate the minor differences between these alternative thresholds, a specific example using real data will be given towards the end of the paper.

In these analyses, the effects examined relate only to the first critical band of hearing, so all data are either band-limited or filtered at 100Hz with an 8-pole low-pass butterworth filter prior to passing through the hearing and threshold processes.

3 SIMULATION RESULTS

A numerical simulation was undertaken in which two band-limited components of sound were introduced into the first critical band. Of these, the first represented infrasonic/very low frequency pseudo-random gaussian noise from 15Hz to 25Hz, at an rms level corresponding to 12dB below the hearing threshold. This noise was maintained at a fixed level throughout.

A second, higher frequency component of random noise was introduced, straddling the bandwidth 50Hz-90Hz. For the sequence of tests its amplitude was progressively increased from -20dB to +6dB relative to the hearing threshold.

Figure 2 shows the $1/3^{\text{rd}}$ octave spectra for these two components of noise, compared directly to the conventional hearing threshold. It can be seen that according to traditional criteria, the infrasonic/low-frequency noise would be considered to be inaudible, while the higher frequency noise would be expected to be just audible.

Figure 3 shows a sequence of four separate plots of high resolution (0.1Hz) frequency spectra. These correspond to introducing the fixed level low-frequency noise, together with the higher frequency noise at four separate levels of -20dB, -6dB, 0dB and +6dB relative to the hearing threshold. The plots show the signals after passing through the initial hearing simulation filter, but both before and after the threshold process.

The color convention is chosen to correspond to Fig 2, with red representing the constant amplitude low-frequency component, and blue representing the varied amplitude high frequency noise at the input to the threshold. The green trace represents the total output after the threshold process.

Figure 3a shows that when the high frequency component is at -20dB, there is zero output from the threshold process, because all the signals are too low to meet the threshold. But when the high frequency component is increased to -6dB in Fig 3b, a (green) output starts to develop, although as yet it has little distinct character. In Fig. 3c, at 0dB, both the low-frequency and high frequency components clearly emerge, while in Fig. 3d, with the high frequency noise at +6dB, both low-frequency and high-frequency output components have risen to match the levels of their respective inputs, despite the existence of the threshold which would otherwise inhibit the low-frequency component.

To indicate the precision of the infrasonic/low-frequency output signal, Fig. 4 shows the result of time-domain filtering the output, to identify this component alone. The filtering utilized a 6-pole high-pass filter at 10Hz, and an 8-pole low-pass filter at 30Hz, thus embracing both the 15-25Hz low-frequency signal and the immediate side-band noise. As before, the red trace represents the input to the threshold, and the green trace represents the filtered output. It can be seen that the low-frequency signal is very closely reproduced, despite the fact that its level is well below the limits of the threshold.

4 RELATIONSHIP TO PRIOR REPORTS

The possibility that infrasound or very low-frequency sound could be sensed or perceived when it is below the nominal hearing threshold was discussed by Stevens³ et al. who surmised that this might be a result of noise-induced house vibration or local enhancement within a building. An alternative explanation might be that this is a consequence of the effect described above, whereby the presence of very low-level audible noise enhances perception.

More recently, Matsumoto⁴ et al. described laboratory testing where subjects were exposed to three examples of infrasonic and low-frequency random noise with very different amplitudes of the infrasonic component. The relevant spectra are shown in Fig. 5. The test subjects (and those conducting the experiment) could reportedly distinguish between the three different test signals, despite the fact that according to conventional assessment, the differences between all three were well below the threshold of hearing. The authors conjectured that the higher frequency audible components of the test spectra, which were of common value to all three, might in some way be conveying information. The present argument, namely that such higher frequency components can enhance perception of low-frequency noise as a result of interaction induced by the finite threshold, might now provide a more rigorous explanation.

5 WIND TURBINE NOISE WITHIN A RESIDENCE

The impulsive infrasonic component of wind turbine noise measured within a house using a B&K 4193-L-004 infrasonic microphone and recorded on a RION DA-20 digital recorder, is shown as a time-trace in Fig.6. Data were captured at 25.6kHz, and decimated to 1kHz for all subsequent analyses. The frequency spectrum, evaluated with 0.1Hz nominal bandwidth is shown in Fig 7. As commented earlier, the periodic series of very low frequency discrete harmonics should not be considered to be independent components; they can combine

coherently to give significant enhancement, but this is insufficient to bring the levels up to threshold values. The overall spectrum to 100Hz has very similar properties to the preceding examples, having sub-threshold components at the lower end, and taking into account the 0.1Hz resolution, audible components at the upper end of the first critical band.

The time series was filtered using the inverse hearing-threshold filter, and then subjected to the threshold as previously described. It was found that for the threshold amplitude at 0dB, corresponding to the median hearing threshold, the infrasonic component was indistinguishable from threshold noise. When the threshold was reduced by -8dB, which represents the most sensitive decile of young adult hearing, the infrasonic component clearly emerged. The output spectra for a threshold at -8dB and -12dB are shown in Fig 8a and 8b. Once again the red trace represents the input to the threshold process, and the green trace shows the output. In Fig 8a two additional traces are added, corresponding to the alternative threshold definitions of Fig. 1b. It can be seen that this has only a very minor influence on the level of the threshold noise.

It is apparent that for frequencies of 5Hz and above, the spectrum is very largely reproduced at the output. Once again, to illustrate the precision of the infrasonic component, the time-series output was filtered, this time with a 6-pole high-pass filter at 5Hz, and an 8-pole low-pass filter at 20Hz, and the resultant time-traces are shown in Fig 9a and 9b, for thresholds of -8dB and -12dB respectively. The same conventions of red and green are adopted, and it can be seen that the infrasonic time series is convincingly reproduced at the output over this frequency range.

In order to estimate the overall amplitude of the noise introduced by the threshold effect, the clean input signal was subtracted from the threshold output signal to yield the residual threshold noise. This was then filtered over the infrasonic decade 2Hz to 20Hz, and the ratio of signal to threshold noise calculated, for different values of threshold setting. The results are shown in Fig. 10, for a range of threshold settings from 0dB (median) to -12dB (2 standard deviations, corresponding to ~ 2.5% of all adults). It is clear that at 0dB, the threshold noise dominates, but as the threshold is reduced, the signal progressively emerges, so that it may be perceived at -6dB (16% of adults) with an S/N ratio ~ 4dB and subsequently with increasing levels of precision for more sensitive individuals.

6 CONCLUSIONS AND FINAL PERSPECTIVE

Numerical simulation of threshold interaction between higher frequency components and low-frequency components within the first critical band has been undertaken. The model has assumed the top-level characteristics of the known hearing frequency response, together with a simple amplitude constraint on response at the hearing threshold. The resultant interaction has been shown to enhance perception of low-frequency noise and infrasound. The word “perception” has been used, because the analysis indicates that a low-frequency response is likely to be induced in the nerve output signals from the hair cells of the inner ear, but it is not clear how these effects might subsequently manifest themselves. These aspects merit future investigation, but nevertheless an initial perspective can be provided.

In the analysis of section 5, the infrasonic output of the threshold process was filtered using an 8-pole low-pass filter at 20Hz. It should be noted that the *linear* combination of the simulated input transfer function for the hearing response, coupled with an 8-pole, 20Hz low-pass output filter, almost exactly reproduces the G-weighting frequency response which is conventionally used to characterize infrasound. So to enable a more familiar perspective, and to

indicate possible effects, the final Fig. 11 is shown. This shows several different infrasonic time signals, filtered with a linear time-domain filter having a G-weighting characteristic, to compare their respective levels. The results show the logarithmic output amplitude, presented using a conventional dB scale re 2×10^{-5} pascals, to enable an adequate dynamic range of different signals to be compared.

The G-weighted wind-turbine signals both outside and inside the house are shown in blue and green respectively, and compared to two separate reference signals, shown in red. The upper red trace shows the test signal reported by Chen⁵ et al., who subjected 5 young adult test subjects to 2.14Hz infrasound at 110dB SPL, ie 82dBG. They reported that the test subjects experienced adverse effects and increased blood-pressure after 1 hour's exposure, despite the fact that this level is 11dB below the nominal adult threshold at 2.14Hz. In contrast, the lower red trace corresponds to numerical simulation of the G-weighted sound pressure changes experienced by a "child-on-a-swing", also corresponding to 110dB unweighted SPL. (The simulation included non-linear, large amplitude effects, which accounts for the asymmetry of the trace.) This latter example has frequently been used as an argument to dismiss the effects of infrasound, but it can be seen that the resultant dBG levels, at only ~ 50dBG, are puny compared with the dBG levels generated by the wind-turbines.

The dBG levels for the wind-turbine infrasound inside the house are 10-15dB lower than the Chen test signal which gave rise to adverse effects after only 1 hour. But since there is an 8dB increase in sensitivity for 10% of young adults, it is clear that these infrasonic wind turbine levels could be expected to become a problem after several hours of exposure.

6 REFERENCES

1. T.H.Pedersen, "Low Frequency Noise from Large Wind Turbines," Project Report Danish Energy Authority, DELTA Danish Electronics Light & Acoustics, 30th April 2008
2. M.A.Swinbanks, "The Audibility of Low Frequency Wind Turbine Noise", *Fourth International Meeting on Wind Turbine Noise*, Rome Italy, 12-14 April 2011
3. D.G.Stevens, K.P.Shepherd, H.H.Hubbard, F.W.Grosveld, "Guide to the Evaluation of Human Exposure to Noise from Large Wind Turbines", *NASA TM83288*, March 1982
4. Yasunao Matsumoto, Yukio Takahshi, Setsuo Maeda, Hiroki Yamaguchi, Kazuhiro Yamada, & Jishnu Subedi, "An Investigation of the Perception Thresholds of Band-Limited Low Frequency Noises: Influence of Bandwidth", *Journal of Low Frequency Noise Vibration and Active Control*, 2003
5. Chen Yuan, Huang Quibai, Hanmin Shi, "An Investigation on the Physiological and Psychological Effects of Infrasound on Persons", *Journal of Low Frequency Noise Vibration and Active Control*, 2004

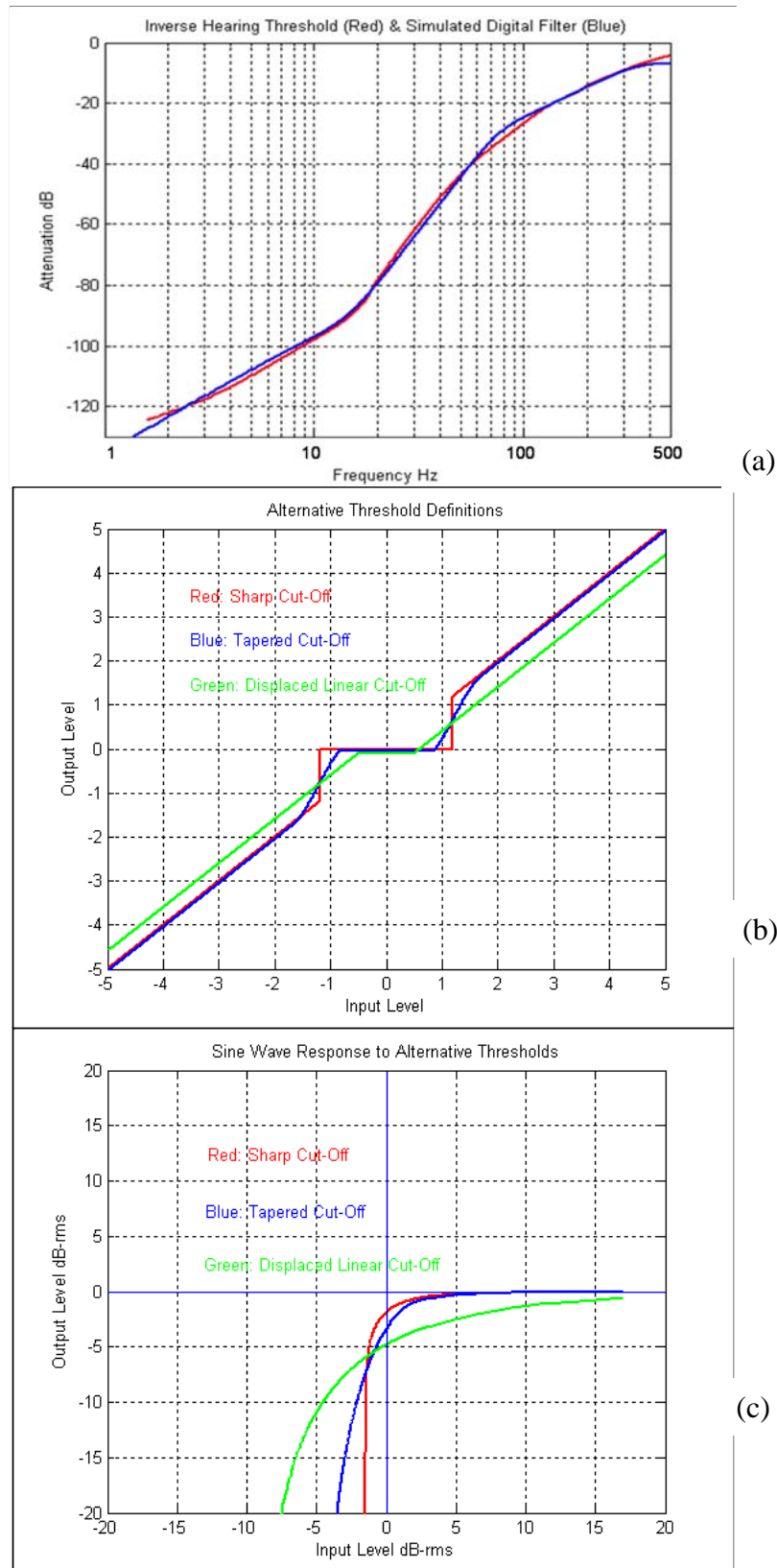


Fig.1 – Simulation Characteristics (a) Frequency response c.f. inverse hearing threshold, (b) Amplitude characteristics of 3 thresholds, (c) Threshold outputs for sine wave input

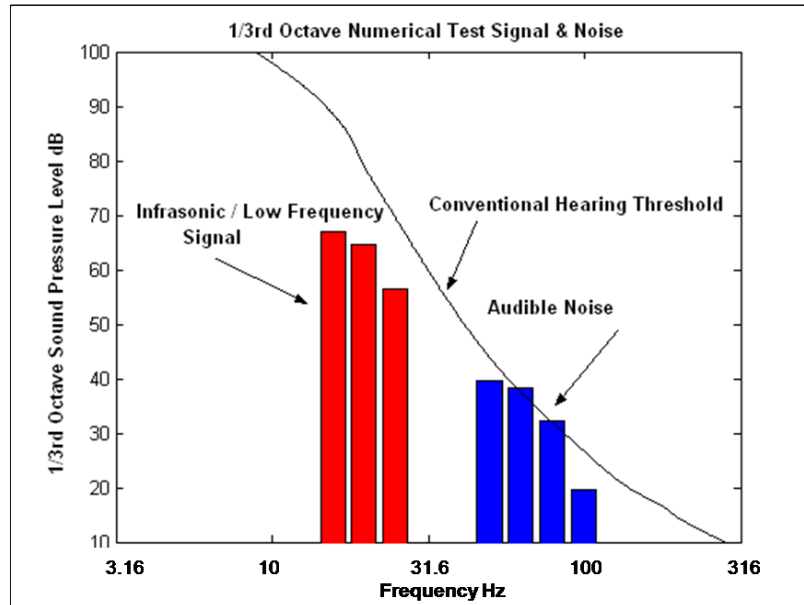


Fig. 2 – 1/3rd octave spectra of infrasonic/low frequency signal & higher frequency noise

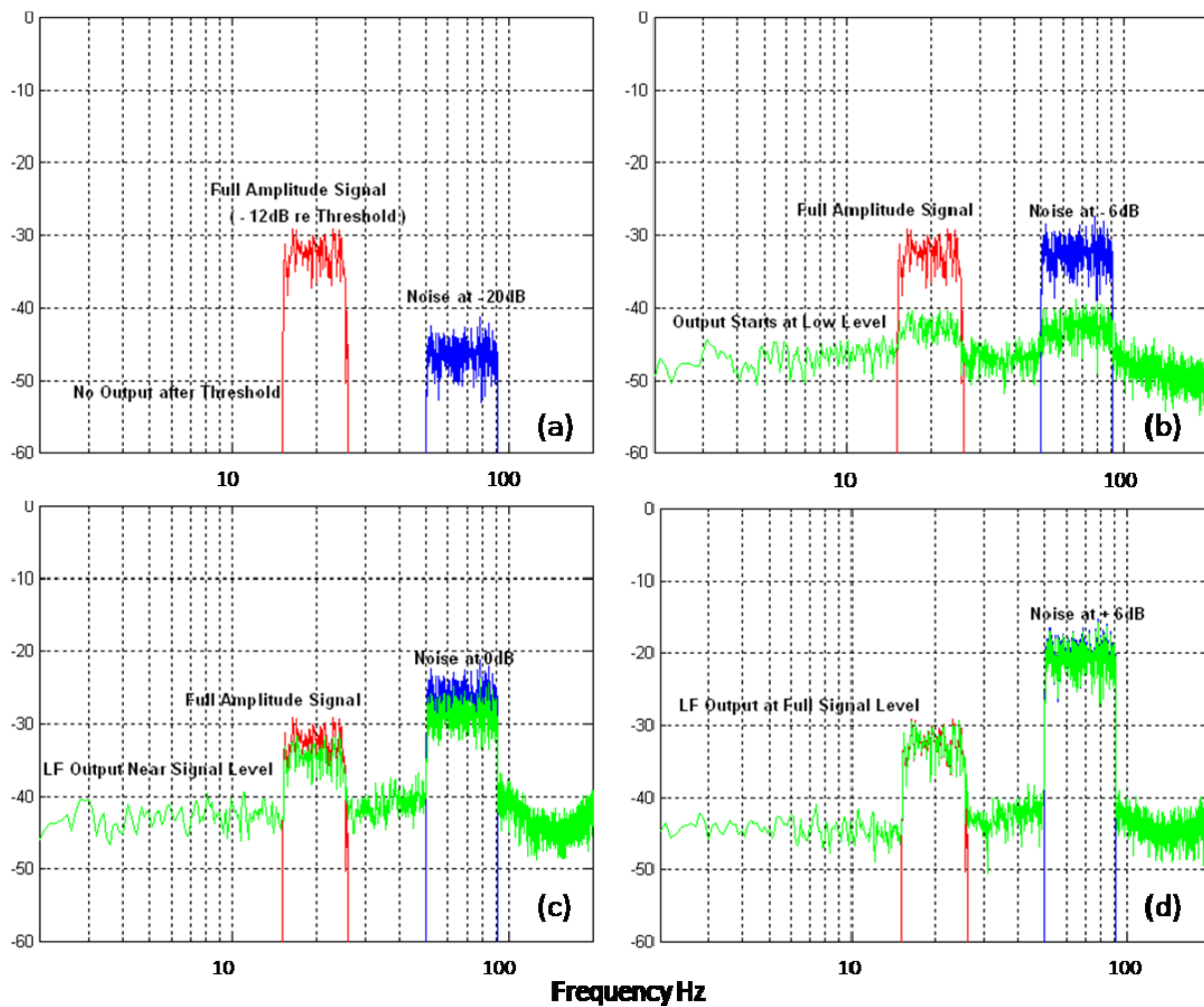


Fig.3 – Effect of progressively increasing h.f. noise (a) -20dB, (b) -6dB, (c) 0dB, (d) +6dB.

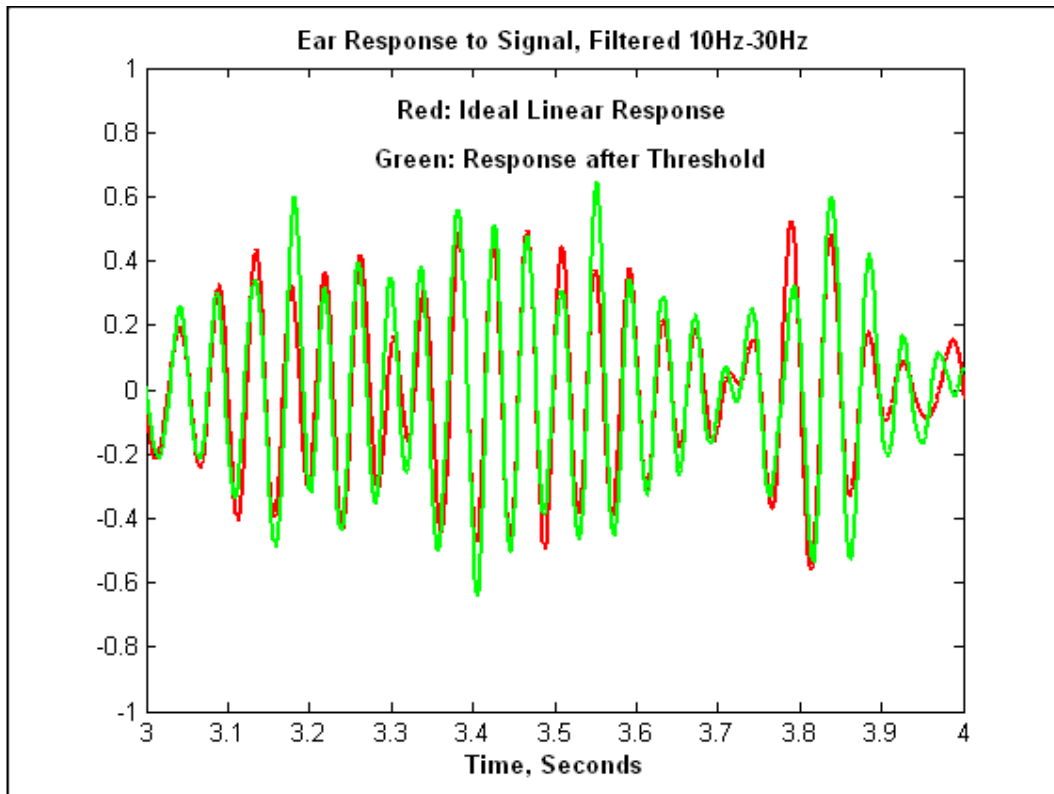


Fig. 4 – Response to signal, filtered 10Hz-30Hz, h.f. noise level at +6dB

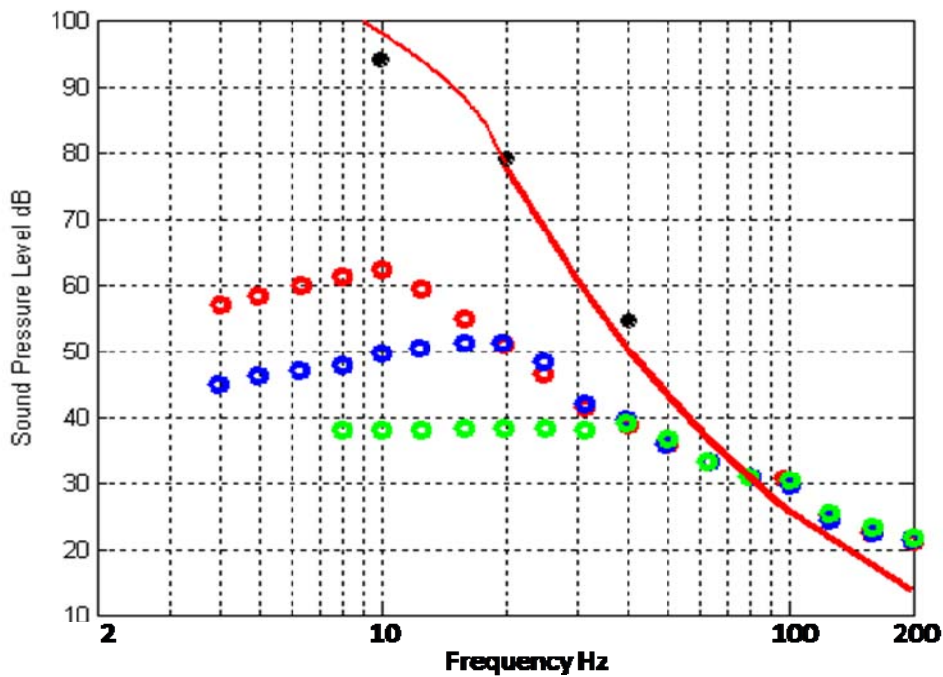


Fig.5 – Median 1/3rd octave spectra (●, ●, ●) for 3 ILFN broadband signals, successfully discriminated. Median thresholds of test subjects, for 3 pure tones ● (after Matsumoto⁴)

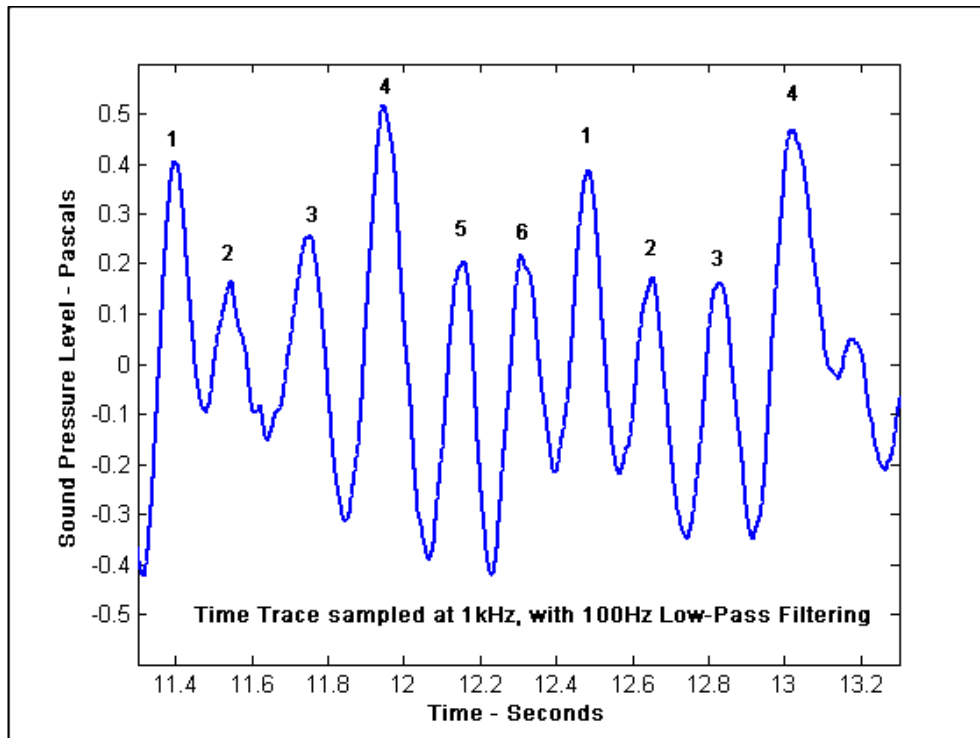


Fig. 6 – Impulsive periodic wind turbine infrasound in bedroom of house. Six separate turbines can be identified. Data filtered to correspond to lowest critical band, peak level 88dB

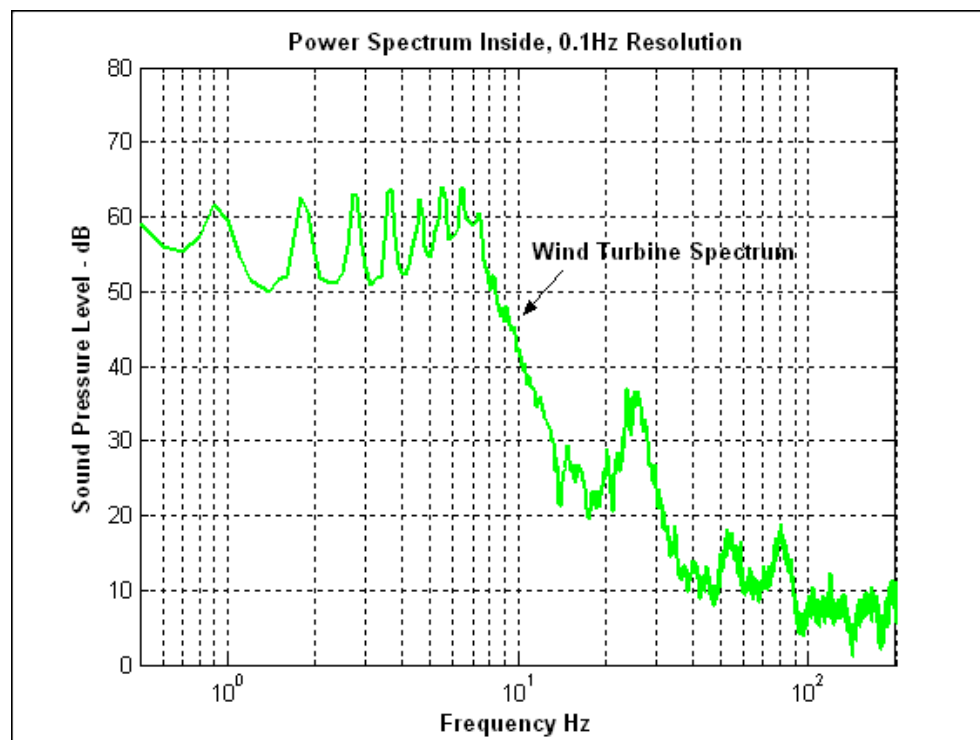


Fig. 7 – 0.1Hz bandwidth power spectrum of unfiltered wind turbine noise in bedroom of house. Impulsive periodic discretely apparent at infrasonic frequencies

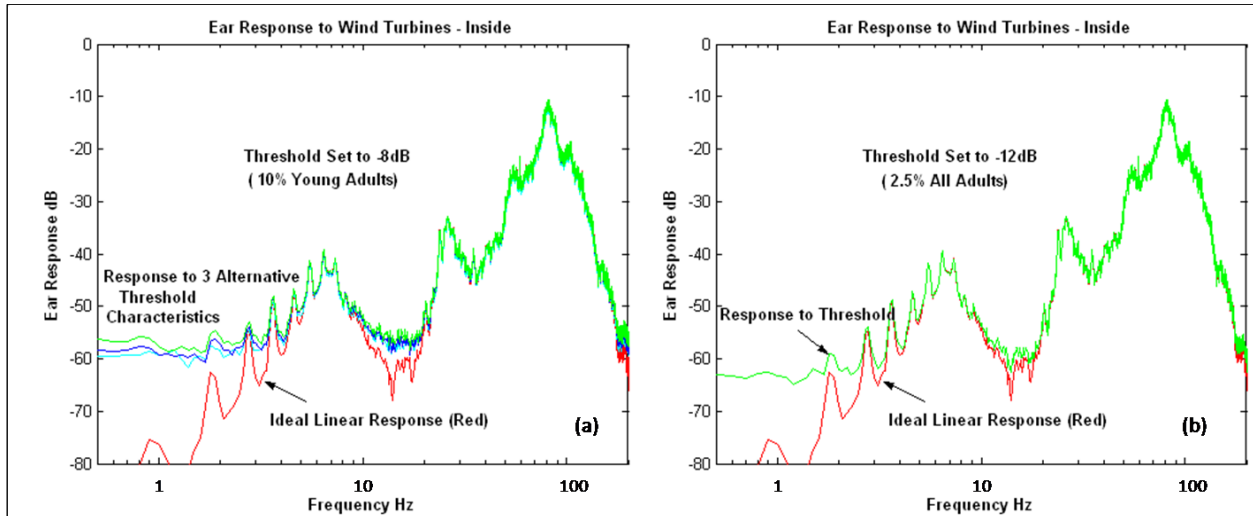


Fig. 8 – 0.1Hz spectra of simulated hearing response to wind turbine noise inside house. Ideal linear response (red) compared to actual output after threshold (green). (a) threshold set to -8dB (10% young adults), with comparison of 3 alternative threshold definitions. (b) threshold set to -12dB (2.5% all adults)

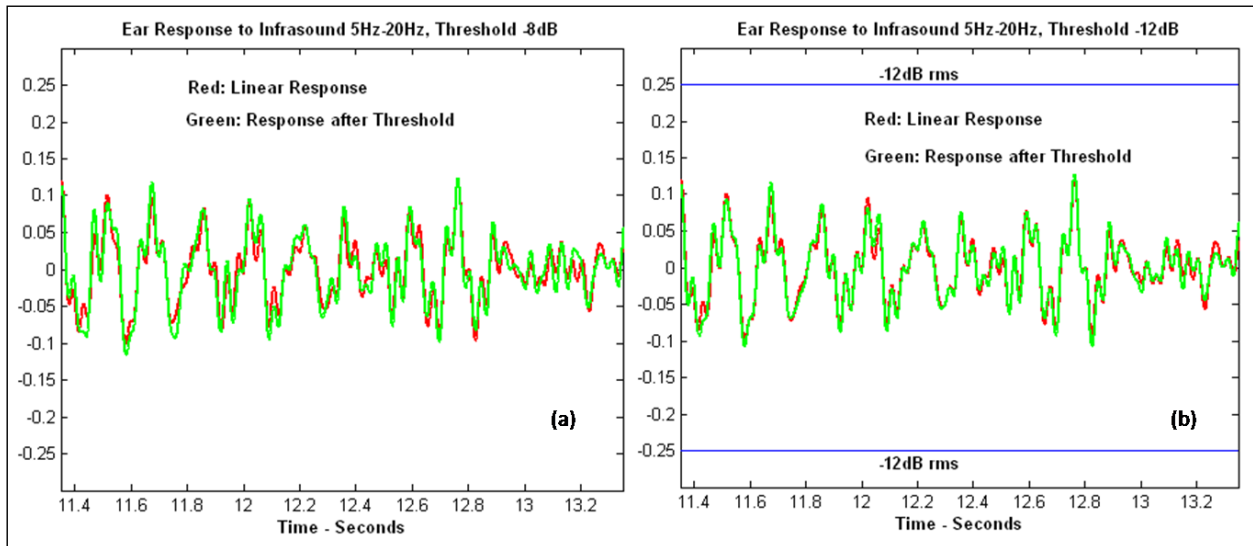


Fig. 9 – Wind turbine time-trace outputs from hearing simulation. Output signals bandpass filtered 5Hz-20Hz. Red - ideal linear response, green - response after threshold. (a) threshold set to -8dB (b) threshold set to -12dB, threshold for -12dB rms shown.

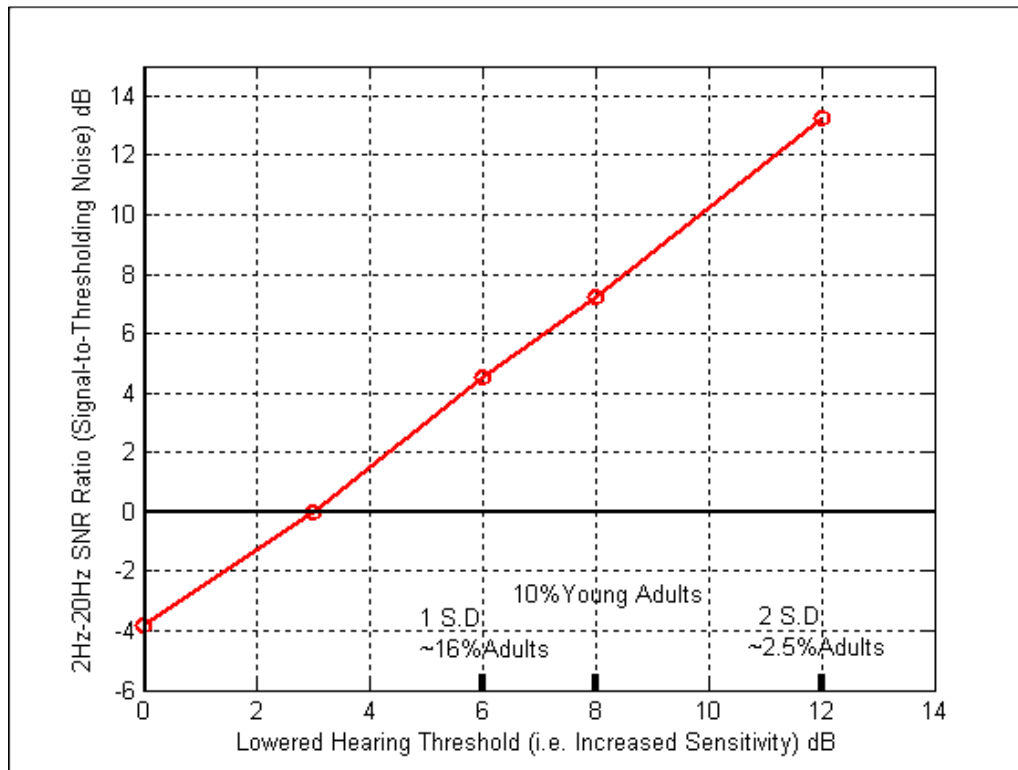


Fig. 10 – Improvement of signal-to-thresholding noise as threshold level is reduced, corresponding to increased sensitivity. Output of threshold filtered over infrasonic decade 2Hz – 20Hz.

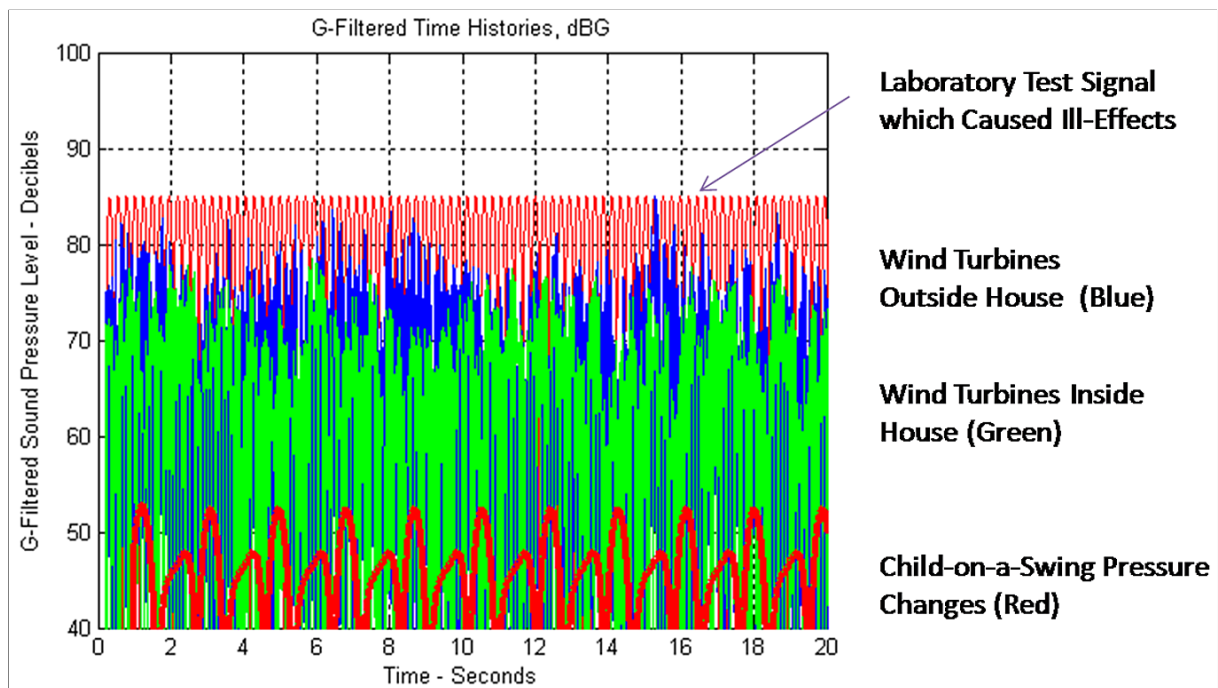


Fig. 11 – Time domain G-weighting filter applied to wind turbine noise, showing comparison with laboratory test signal which reportedly caused ill-effects (Chen⁵), & “child-on-a-swing infrasound” which is clearly lower than any relevant response